Supporting information

Electro-exfoliated PdTe$_2$ nanosheets for enhanced methanol electrooxidation performance in alkaline media

Jingjing Luo,[a] Peng Jiang,[ab] Dongdong Wang,[b] Xueyou Yuan,[c] Hongli Sun,[a] Lang Gan,[a] Chenliang Su,[a] Qitao Zhang,*[a]

[a]*International Collaborative Laboratory of 2D Materials for Optoelectronic Science & Technoogy, Engineering Technology Research Center for 2D Materials Information Functional Devices and Systems of Guangdong Province, Institute of Microscale Optoeletronics, Shenzhen University, Shenzhen 518060, China*

[b]*School of Chemistry and Materials Science, University of Science and Technology of China, Hefei 230027, China*

[c]*Department of Energy Engineering and Venture Business Laboratory, Nagoya University, Nagoya 464–8603, Japan*

Experimental section

Chemicals and Reagents

Palladium (Pd) powders (99.999%) and tellurium (Te) powders (99.95%) were purchased from Alfa Aesar. Tetramethylammonium tetrafluoroborate (BF_4TMA, 98%), propylene carbonate (PC, 98%), methanol (CH_3OH, 98%), ethanol (CH_3CH_2OH, 98%) and potassium hydroxide (KOH, 99.5%) were provided from Macklin. Commercial Pd/C (10 wt%) were got from Innochem (Beijing) Technology Co., Ltd.. Nafion solution (5 wt%) was supplied by Sigma Aldrich.

Synthesis of PdTe$_2$ nanosheets (PTNS)

The $PdTe_2$ bulk was grown via the conventional chemical vapor transport (CVT) method mentioned in our previous work [1]. Then, the cathodic exfoliation procedure was operated under a two-electrode system with direct voltage of −20 V, in which $PdTe_2$ bulk, Pt wire and 0.25 M BF_4TMA solution in PC was employed as working electrode, counter electrode and electrolyte, respectively. After intercalation and washing, black $PdTe_2$ nanosheets were obtained.

Preparation of catalyst inks

All the as-obtained catalysts were used without additional conductive carbon. 2 mg of catalyst was dispersed in a mixed solution consisted 400 μL of ethanol and 30 μL of Nafion. The final ink was obtained after violent sonication for 30 min.

Characterizations

The phase information of samples was characterized on a Rikagu SmartLab X-ray diffractometer (XRD) using Cu Kα radiation (λ = 1.5406 Å). The high-angle annular dark-field scanning transmission electron microscopy (HAADF-STEM), high-resolution transmission electron microscope (HRTEM) and energy dispersive X-ray spectrometry (EDS) mapping images were carried out on a Titan Cubed Themis G2 300 FEI with an acceleration voltage of 300 kV. The chemical states on the surface of samples were investigated via the Thermo Scientific K-Alpha+ with Al Kα microfocus monochromatic source. The total binding energies were calibrated with C1s peak (284.8 eV) as the standard. The molecular vibration and rotation of samples were

recorded by the HORIBA Scientific LabRAM HR Evolution with laser excitation of 532 nm at room temperature. The element content of Pd and Te were measured through inductively coupled plasma mass spectrometry (ICP-MS). AFM characterization was carried out with Bruker Multimode 8 system.

Electrochemical Measurements

The methanol oxidation reaction (MOR) performance of as-obtained PdTe$_2$ nanosheets was investigated using a typical three-electrode system with rotating disk electrode on a CHI760e electrochemical workstation (Chenhua Co., Shanghai, China). A glass carbon electrode (GCE, 5 mm diameter), a platinum wire and an Ag/AgCl electrode were applied as the working electrode, the counter electrode and the reference electrode, respectively. 5 µL of the catalyst ink was deposited on the working electrode for electrochemical measurement. Prior to MOR measurement, all the electrolytes were flushed with nitrogen (N$_2$) for 20 min to remove oxygen and other gases. Cyclic voltammograms (CVs) were performed in 1 M KOH solution and 1 M KOH + 1M CH$_3$OH solution with a scan rate of 50 mV s^{-1} in the potential window of -0.63 and 0.33 V (vs. Ag/AgCl) at room temperature. Electrochemical active surface area (ECSA) was calculated based on the equation of $\mathrm{ECSA} = Q/(m * C)$ in 1 M KOH electrolyte, where Q is the amount of charge needed to reduce PdO to Pd on the surface of catalyst, m is the Pd atomic mass of catalyst deposited on the surface of GCE, and C is the theoretical amount of charge needed to reduce a layer of PdO to Pd (420 µC cm^{-2}). CVs in 1 M KOH containing 1M CH$_3$OH solution at various scan rates were also recorded to further analyze the dynamic process. The electrocatalytic activities of these as-obtained catalysts were evaluated by their mass activities and specific activities that normalized the current to the loading amount of Pd and ECSA, respectively. The stability of these catalysts was estimated by chronoamperometry (CA) experiment in 1 M KOH + 1 M CH$_3$OH solution at -0.3 V vs. Ag/AgCl for 7200 s. The Tafel plots were obtained by the equation of $\eta = a + b\log(j)$, where η is the overpotential, j is the current density, a is a constant and b is the slope of the plot. The electrochemical impedance spectra (EIS) were performed at a frequency range between 100 kHz and 0.1 Hz with an amplitude of 5 mV. The CO-stripping tests were executed by holding the working electrode at -0.8 V vs Ag/AgCl for 15 min in the CO-saturated 1 M KOH solution. Subsequently, the excess CO in the electrolyte was purged out with N$_2$ for 15

min. Then the CO stripping CVs were recorded for two cycles between -0.8 and 0.3 V vs Ag/AgCl at a scan rate of 50 mV s^{-1}. Converted potentials were used in all figures referred to the reversible hydrogen electrode (RHE) by the equation of $E_{(RHE)} = E_{(Ag/AgCl)} + 0.1976 + 0.0596 \times 14$.

Computational methods

All the density functional theory (DFT) calculations were performed by the Vienna Ab Initio Package (VASP) [2, 3] within the generalized gradient approximation (GGA) using the PBE formulation [4]. The ionic cores were described by the projected augmented wave (PAW) potentials [5, 6]. The valence electrons were taken into account by the means of the plane wave basis with a kinetic energy cutoff of 450 eV. Partial occupancies of the Kohn−Sham orbitals were allowed using the Gaussian smearing method and a width of 0.05 eV. The electronic energy was considered self-consistent when the energy change was smaller than 10^{-4} eV. Geometry optimization was considered convergent when the force change was smaller than 0.03 eV/Å. Grimme's DFT-D3 methodology was used to describe the dispersion interactions [7]. The vacuum spacing perpendicular to the plane of the structure is 15 Å. The Brillouin zone integral uses the surfaces structures of 2×2×1 monkhorst pack K point sampling. Finally, the adsorption energies (E_{ads}) are calculated by the equation of $E_{ads} = E_{ad/sub} - E_{ad} - E_{sub}$, where $E_{ad/sub}$, E_{ad} and E_{sub} are the optimized adsorbate / substrate system, the adsorbate in the structure and the clean substrate, respectively.
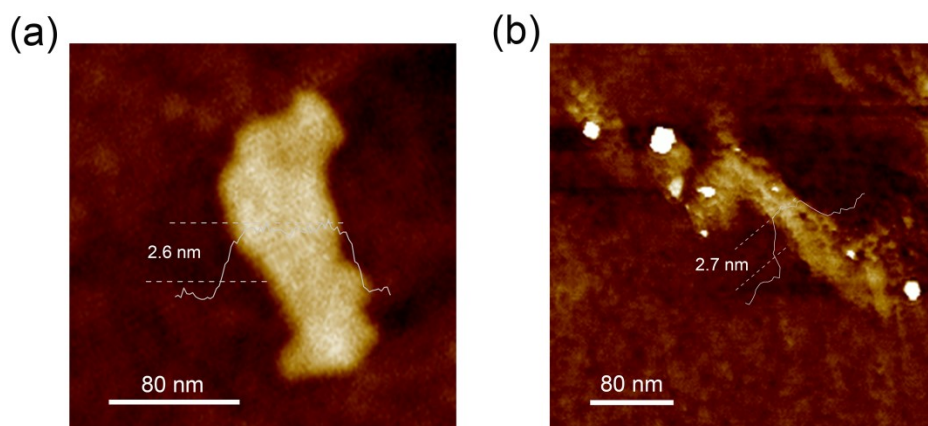
(a)

2.6 nm

80 nm

(b)

2.7 nm

80 nm

Fig. S1 AFM image of PTNS (a) before and (b) after electrooxidation reaction.

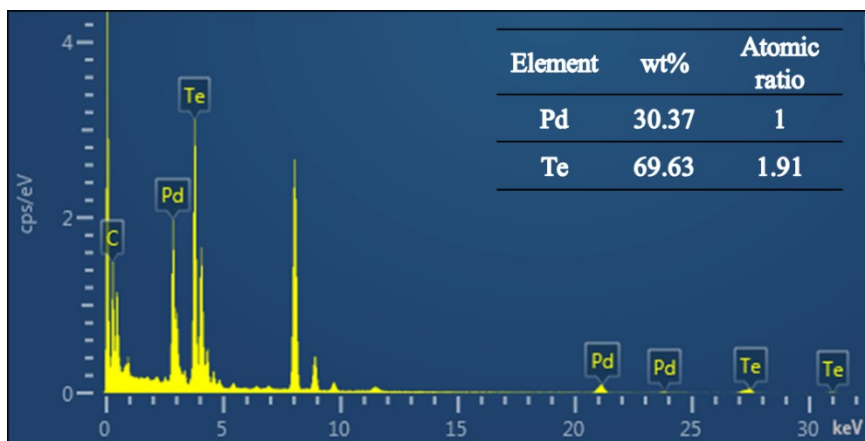| Element	wt%	Atomic ratio
Pd	30.37	1
Te	69.63	1.91

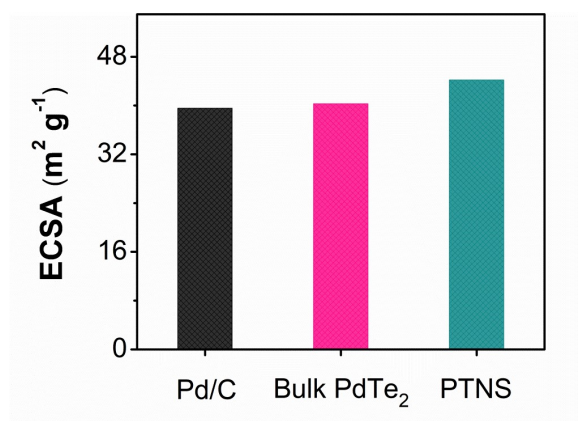Fig. S2 Energy dispersive X-ray spectrometry (EDS) analysis date of PTNS.

Fig. S3 ECSAs of PTNS, bulk $PdTe_2$, and commercial Pd/C.

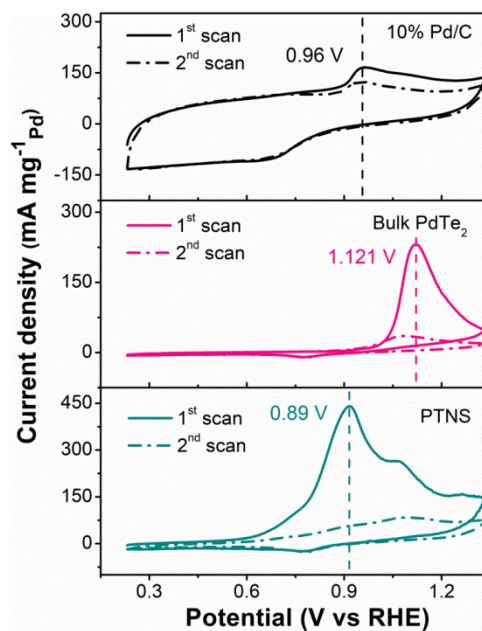Fig. S4 CO stripping curves of PTNS, bulk PdTe$_2$, and commercial Pd/C in 1 M KOH solution at a scan rate of 50 mV s^{-1}.
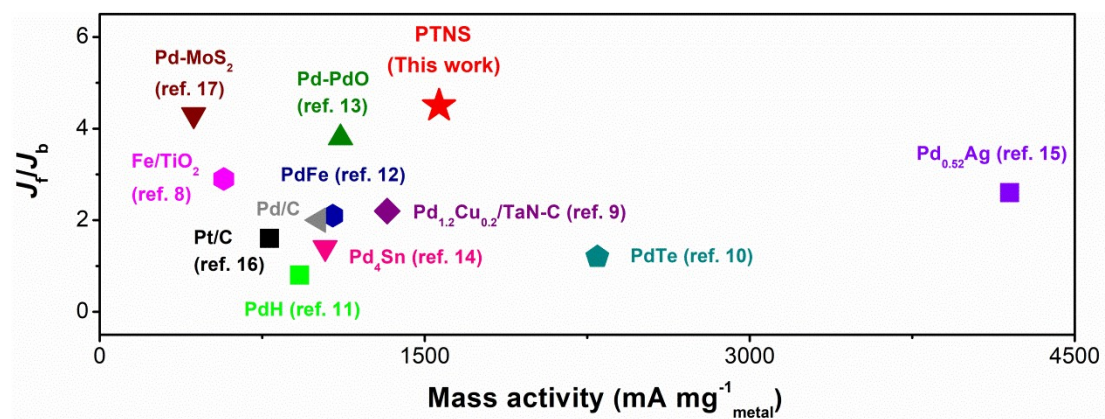

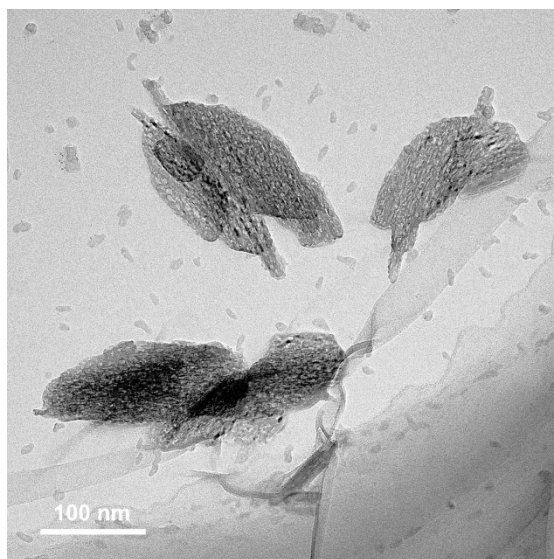Fig. S5 Comparison between PTNS and the reported catalysts toward MOR in alkaline solution.

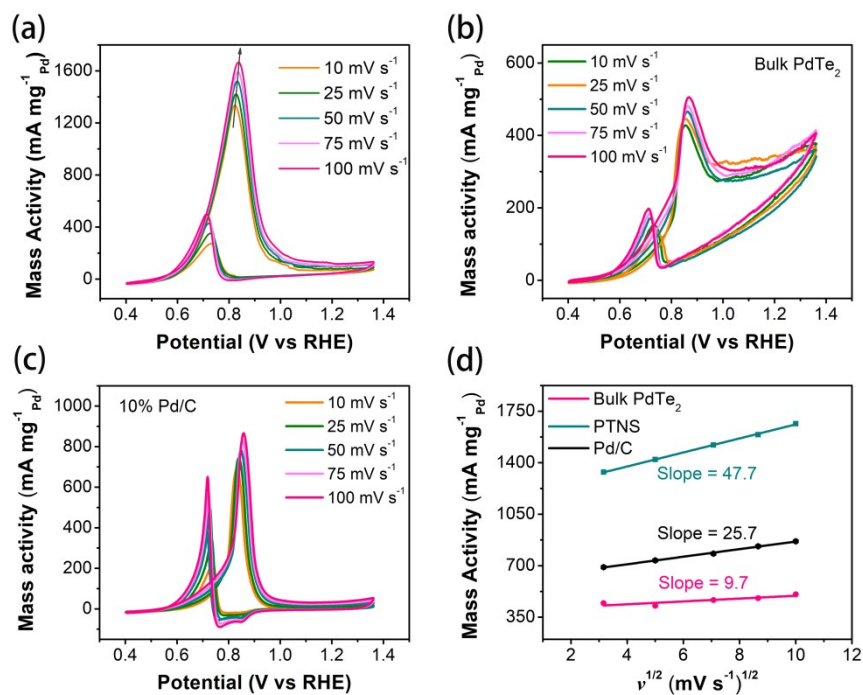Fig. S6 TEM image of PTNS after electrooxidation reaction.

Fig. S7 CV curves of (a) PTNS , (b) bulk $PdTe_2$ and (c) commercial Pd/C in 1 M KOH containing of 1 M CH_3OH solution at 10, 25, 50, 75, and 100 mV s^{-1}.
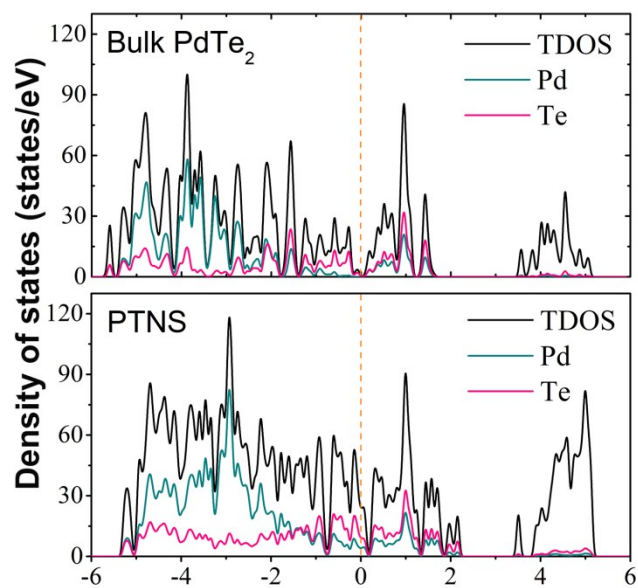
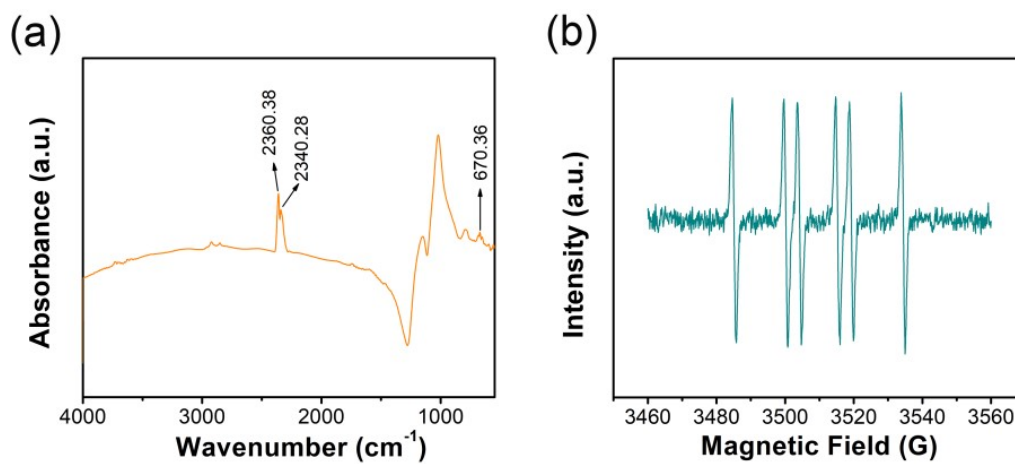Fig. S8 The total density of states (TDOS) of PTNS and bulk PdTe$_2$.

Fig. S9 (a) The FTIR absorption spectrum of PTNS and (b) the ESR spectrum of electrolyte after electrooxidation process.
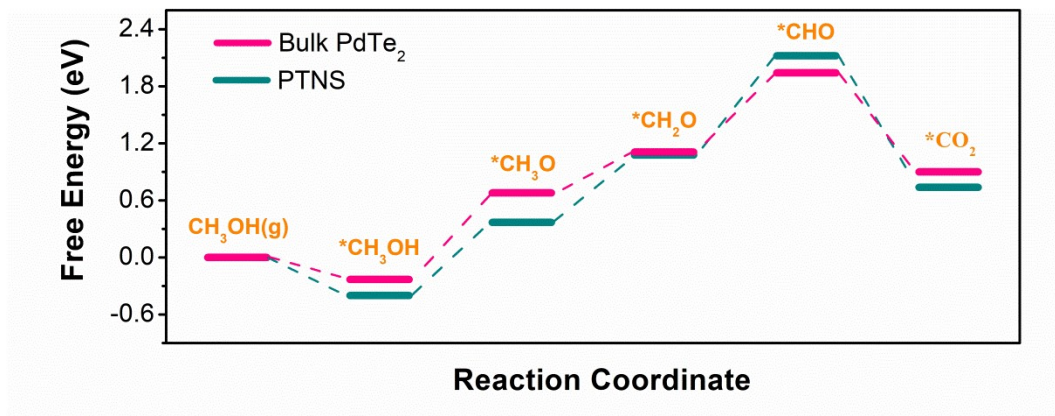
Fig. S10 The potential energy profiles of methanol oxidation for PTNS and bulk $PdTe_2$.

Table S1 The ratios of forward and backward current density of PTNS, bulk $PdTe_2$ and Pd/C catalysts.

Catalysts	Forward current density (J_f) (mA mg$^{-1}_{Pd}$)	Backward current density (J_b) (mA mg$^{-1}_{Pd}$)	J_f/J_b
Commercial Pd/C	783.8	494.9	1.6
Bulk $PdTe_2$	470.9	137.1	3.4
PTNS	1566.4	347.8	4.5

References

1   J. J. Luo, M. J. Fan, L. W. Xiong, Q. Y. Hao, M. N. Jiang, Q. J. He and C. L. Su, *ACS Appl. Mater. Inter.*, 2021, **13**, 27963-27971.

2   G. Kresse and J. Furthmüller, *Phys. Rev. B*, 1996, **54**, 11169-11186.

3   J. P. Perdew, K. Burke and M. Ernzerhof, *Phys. Rev. Lett.*, 1996, **77**, 3865-3868.

4   G. Kresse and D. Joubert, *Phys. Rev. B*, 1999, **59**, 1758-1775.

5   P. E. Blöchl, *Phys. Rev. B* 1994, **50**, 17954-17979.

6   S. Grimme, J. Antony, S. Ehrlich and H. Krieg, *J. Chem. Phys.*, 2010, **132**, 154104.

7   G. Henkelman, B. P. Uberuaga and H. Jonsson, *J. Chem. Phys.*, 2000, **113**.

8   Y. J. Yu, J. X. Yang, X. L. Wang, B. L. Wang and S. J. Hu, *Surf. Interfaces*, 2021, **25**, 101231.

9   N. Ye, Y. X. Bai, Z. Jiang and T. Fang, *Electrochim. Acta*, 2021, **383**, 138365.

10   W. Qiao, X. D. Yang, M. Li and L. G. Feng, *Nanoscale*, 2021, **13**, 6884-6889.

11   X. Y. Guo, Z. Hu, J. X. Lv, J. q. Qu and S. Hu, *Dalton Trans.*, 2021, **50**, 10359-10364.

12   H. Xu, H. Y. Shang, C. Wang, L. J. Jin, C. Y. Chen and Y. K. Du, *Nanoscale*, 2020, **12**, 2126-2132.

13   T. J. Wang, F. M. Li, H. Huang, S. W. Yin, P. Chen, P. J. Jin and Y. Chen, *Adv. Funct. Mater.*, 2020, **30**, 2000534.

14   Y. Zhang, B. L. Huang, Q. Shao, Y. G. Feng, L. K. Xiong, Y. Peng and X. Q. Huang, *Nano Lett.*, 2019, **19**, 6894-6903.

15   L. Huang, J. S. Zou, J. Y. Ye, Z. Y. Zhou, Z. Lin, X. W. Kang, P. K. Jain and S. W. Chen, *Angew. Chem. Int. Ed.*, 2019, **58**, 8794-8798.

16   Z. C. Zhang, Z. M. Luo, B. Chen, C. Wei, J. Zhao, J. Z. Chen, X. Zhang, Z. C. Lai, Z. X. Fan, C. L. Tan, M. T. Zhao, Q. P. Lu, B. Li, Y. Zong, C. C. Yan, G. X. Wang, Z. C. J. Xu and H. Zhang, *Advanced materials*, 2016, **28**, 8712-8717.

17   L. H. Yuwen, F. Xu, B. Xue, Z. M. Luo, Q. Zhang, B. Q. Bao, S. Su, L. X. Weng, W. Huang and L. H. Wang, *Nanoscale*, 2014, **6**, 5762-5769.